Joint Pathology Center
Veterinary Pathology Services

WEDNESDAY SLIDE CONFERENCE 2024-2025

Conference #17 — 22 January 2025

CASE I:

Signalment:
Seven-year-old, male rhesus macaque, *Macaca mulatta*.

History:
Euthanasia was due to chronic, progressively worsening diarrhea.

Gross Pathology:
The macaque was in very lean nutritional condition. Liver was firmer than normal, and the common bile duct was dilated and tortuous. Visceral lymph nodes of the abdomen were enlarged, soft and confluent. Large intestines had mucosal thickening.

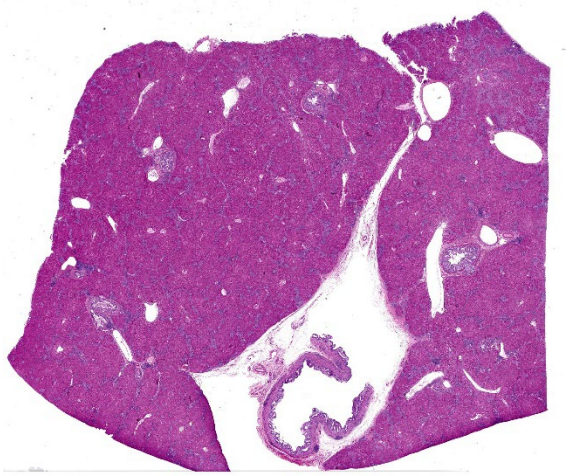

Figure 1-1. Liver, rhesus macaque. At subgross magnification, bile ducts are hyperplastic and there is bridging portal fibrosis. (HE, 7X)

Laboratory Results:
PCR: 1) Common bile duct: Enterocytozoon bieneusi positive; Cryptosporidium negative.

2) Mesenteric lymph node, spleen and ileum: Mycobacterium negative

Bacteriology: Colon: Colon: E. coli, Klebsiella pneumoniae, Proteus vulgatus, Streptococcus viridans group, & Lactobacillus spp present. Strict Anaerobes: Prevotella oris & Peptoniphilus asaccharolyticus present.

Microscopic Description:
Large intrahepatic bile ducts and the common bile duct had moderate, diffuse mucosal hyperplasia with moderate lymphocytic and plasmacytic inflammation. Portal triads were expanded by similar inflammation and bridging fibrosis is present. Gram stains revealed small colonies of 1-2 µ, gram positive organisms, typically in sloughed biliary epithelium.

The liver had numerous granulomas in all lobes. Granulomatous inflammation was also present in spleen intestines and axillary and mesenteric lymph nodes. Acid fast stain of liver sections revealed small numbers of acid-fast positive bacilli within granulomas. The ileum had sheets of epithelioid macrophages with myriad intracytoplasmic acid-fast bacteria.

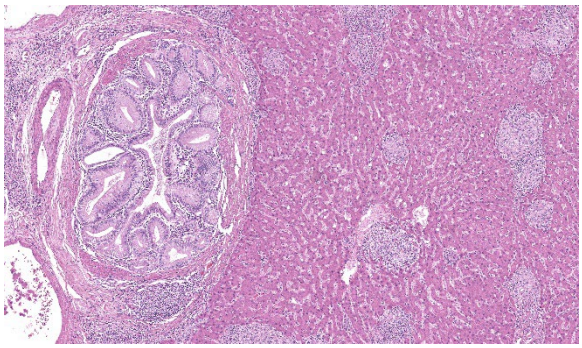

Figure 1-2. Liver, rhesus macaque. The lining of bile ducts is markedly hyperplastic and the lamina propria is infiltrated by moderate numbers of lymphocytes and plasma cells. There is biliary hyperplasia and bridging portal fibrosis. There are numerous small granulomas scattered throughout the hepatic parenchyma. (HE, 110X)

Contributor's Morphologic Diagnosis:
Liver: Cholangiohepatitis, hyperplastic, chronic. diffuse, moderate with intracellular protozoa, Enterocytozoon bieneusi.

Liver: Granulomatous hepatitis, moderate, multifocal (Mycobacterium avium complex, presumptive.)

Contributor's Comment:
Enterocytozoon bieneusi (EB) is a microsporidian parasite that is frequently associated with diarrhea and biliary disease in SHIV and SIV infected macaques. It also is a common cause of chronic diarrhea in human HIV patients. EB isolates are divided into 11 groups and numerous subgroups based on polymorphisms of *ribosomal internal transcribed scribed spacer* DNA. (ITS).[5] Most laboratory primates have organisms from Group 1, subgroup D which is the common strain that affects humans. Wild and zoo apes and monkeys have EB isolated from different groups and/or subgroups. Transmission is likely direct with organisms having been isolated in water and fresh produce. They have also been isolated from mollusks.[3,4]

EB spores have been isolated from the feces of immunocompetent animals.[6] Experimental infection of immune competent macaques by spores of human origin resulted in fecal shedding in about 8 weeks with infections persisting for months, and elevation of ALK but not ALT, GGT, or AST serum liver enzymes. Spores were isolated from bile and feces, but other developmental stages were not found and symptoms were not observed. Histology of the biliary tree of immunocompetent macaques had lymphoplasmacytic cholecystitis and choledochitis.[2]

Once infected, immunocompromised animals frequently develop symptoms concurrent with a drop in T4 (CD4) lymphocyte counts. If the T4 count remains stable, immunodeficient animals can remain asymptomatic.[2] In immune suppressed animals, infection results in hyperplastic cholecystitis and choledochitis with lymphoplasmacytic inflammatory infiltrates. Though EB is associated with diarrhea, coinfections are common so the contribution of EB to clinical signs is often uncertain. All stages of the organism can be identified by *in situ hybridization* in mucosal cells of the biliary tree, duodenum, and jejunum. Plasmodia are multinucleated; they and sporoblasts measure between 4-12 um. Spores

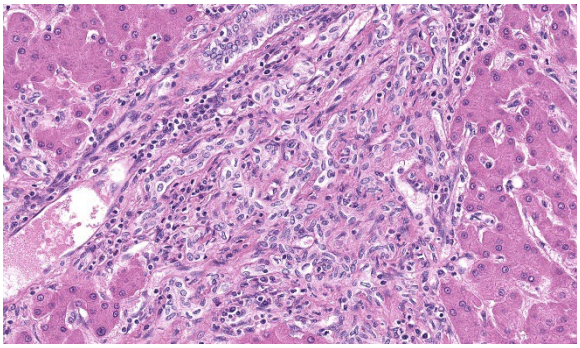

Figure 1-3. Liver, rhesus macaque. There is marked biliary hyperplasia and fibrosis expanding portal triads. (HE, 457X)

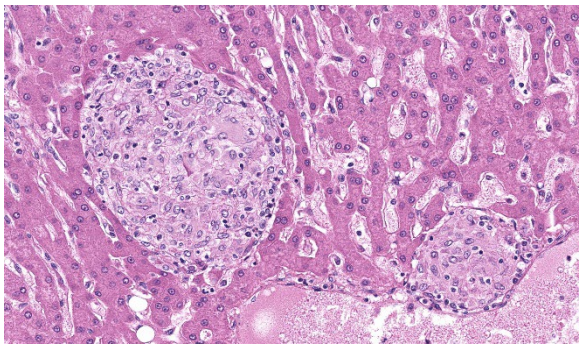

Figure 1-4. Liver, rhesus macaque. Numerous poorly formed granulomas composed of large numbers of spindled epithelioid macrophages are scattered throughout the parenchyma. (HE, 478X)

and sporoblasts measuring 0.8-1.5 um can be visualized in sloughed biliary mucosal cells by using either Ziehl-Neelson acid-fast, Brown and Hopps, Weber's modified trichrome, or methenamine silver stains. Only small numbers of organisms are found this way.[2,6,7] Differential diagnoses include another microsporidian organism, *Cryptosporidium parvum*, and ascending bacterial infections.[7]

As microsporidia rely on host cells for nucleotides and amino acids, they are considered obligate pathogens.[1] Although originally classified as protozoa, they have since been placed in a separate phylum and are thought to closely related to fungi due to protein and structural analysis, and *simple sequence repeat RNA* (SSR) gene sequencing. They are characterized by chitinous spore walls, coiled polar tubules and a radiolucent vacuole and mitochondria-like organelles that lack mitochondrial genome.[1] After ingestion, spores attach to host cell membranes using the polar tubule through which the sporoplasm enters host cell cytoplasm. It then becomes a meront which divides into plasmodia and through sporogony form sporoblasts that mature into spores.[3,4] Studies on *Encephalitozoon*, another microsporidian organism, have found that immunity is depended on CD8 lymphocytes, IFN-gamma and IL-12.[3]

A commonly associated opportunistic coinfection with EB is atypical mycobacteriosis also referred to a non-tuberculous mycobacterium (NTM). NTM are thought to be acquired from either soil or water. Species of the *Mycobacterium avium-intracellulare* species complex (MAC) are most frequently identified. Infections are characterized by diffuse granulomatous enterocolitis with large numbers of intracellular bacteria. Disseminated disease also can occur with fewer organisms present in other organs which is the is the pattern of this case. Another common NTM species is *M. kansasii* which can be present asymptomatically. *M genevense*, is a species isolated in human HIV patients causes lesions that are similar to MAC with numerous bacteria. One study found that animals were more likely to have symptoms from NTM when coinfections are present.[8,10]

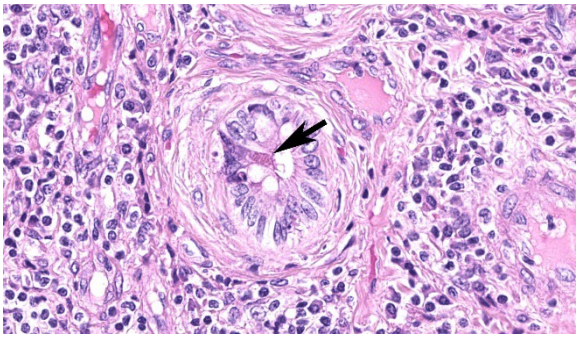

Figure 1-5. Liver, rhesus macaque. Rare biliary epithelial cells contain cytoplasmic microsporidian spores.

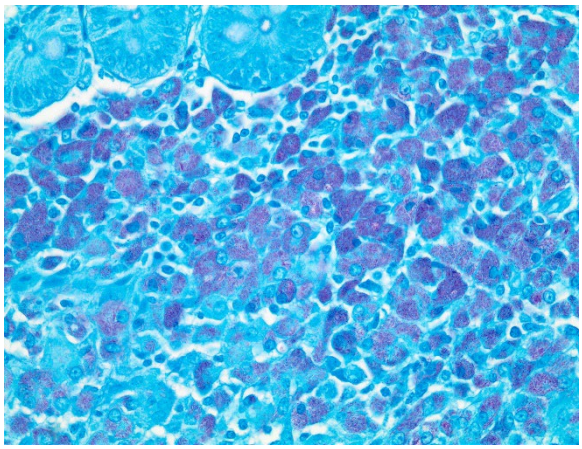

Figure 1-6. Intestine, rhesus macaque. Epithelioid macrophages within the lamina propria contain numerous cytoplasmic acid-fast bacilli. (Ziehl-Neilson, 600X) (*Photo courtesy of:* National Institutes of Health, Bethesda, MD)

The reason for the negative mycobacteria PCR results in the presence of numerous bacteria in this case is uncertain. One lab found a 45.1%% sensitivity with PCR compared to culture.[9] A source of false negative results with PCR are interfering materials such has immunoglobulin and collagen.[11]

Contributing Institution:
National Institutes of Health, ORS

JPC Diagnosis:
1. Liver: Cholangiohepatitis, proliferative and lymphoplasmacytic, chronic, diffuse, moderate, with bridging portal fibrosis and intraepithelial microsporidia.

2. Liver: Hepatitis, granulomatous, multifocal, moderate.

JPC Comment:
This week's moderator is LTC Erica Barkei, JPC's Chief of Resident Training and Education.

In this section, microsporidia are occasionally visible on H&E and special stains, particularly within sloughed biliary epithelial cells. In this section, mycobacterial "granulomas" do have epithelioid and/or multinucleate giant cell macrophages, but lack surrounding lymphocytes and fibrosis and a central core of necrosis as is typical for Th1 granulomas. As the contributor notes, macrophages containing non-tuberculous mycobacteria typically have fewer cytoplasmic organisms outside of the colon, which may reflect the relatively limited degree of granuloma development within the liver seen in this case.

There are several other important diseases of immunosuppressed macaques to consider (although not in this section.) As the contributor notes, *Cryptosporidium* may also be seen within the biliary tract, though this causes suppurative inflammation which is noticeably absent in section. Cytomegalovirus (CMV) has characteristic intranuclear viral inclusions and is also necrotizing. Other common co-infections include simian virus 40 (SV40), *Candida albicans*, *Pneumocystis carinii,* and *Toxoplasma gondii*.

References:

1. Dean P, Hirt RP, Embley TM. Microsporidia: Why make nucleotides if you can steal them? *PLOS Pathogens* 2016; 12(11): e1005870.
2. Green LC, Didier PJ, Bowers, L C. et al. Natural and experimental infection of immunocompromised rhesus macaques (*Macaca mulatta*) with the microsporidian *Enterocytozoon bieneusi* genotype D. *Microbes and Infection* 6 (2004) 996–1002
3. Han B, Weiss LM. Microsporidia: Obligate intracellular pathogens within the fungal kingdom. *Microbiol Spectr*. Author manuscript available in PMC 2017 October 1
4. Li W, Feng Y, Xiao L. Parasite of the month: *Enterocytozoon*. *Trends in Parasitology*, 2021, 20(20):1-2

5. Li W, Feng Y, Santin M. Host Specificity of Enterocytozoon bieneusi and public health implications. *Trends in Parasitology.* 2019, 35(6):436-451
6. Mansfield K, Carville A, Herbert D, et al. Localization of persistent *Enterocytozoon bieneusi* Infection in normal rhesus macaques (*Macaca mulatta*) to the hepatobiliary tree. J Clinical Microbiol. 1998, 36(8): 2336–2338
7. Mansfield K, Carville A, Shevetz D, et al. Identification of an *Enterocytozoon bieneusi*-like microsporidian parasite in Simian-Immunodeficiency-Virus-Inoculated macaques with hepatobiliary disease. *Am J of Path*.1997,150(4): 1395-1405
8. Maslow J, Brar I, Smith G, et al. Latent infection as a source of disseminated disease caused by organisms of the *Mycobacterium avium Complex* in Simian Immunodeficiency Virus–Infected Rhesus Macaques. *Journal of Infect Dis.* 2003; 187:1748–55
9. Park JS, Choi J, Lim, J, et al. The combination of real-time PCR and HPLC for the identification of non-tuberculous mycobacteria. *Ann Lab Med*. 2013, 33:349-352
10. Procop G. HIV and mycobacteria. *Seminars in Diagnostic Pathology*, 34(2017) 332-339.
11. Sidstedt M, Rådström P, Hedman J. PCR inhibition in qPCR, dPCR and MPS mechanisms and solutions. *Analytical and Bioanalytical Chem*. 2020, 412:2009–2023

CASE II:

Signalment:
Adult, male, Ezo raccoon dog (*Nyctereutes procyonoides albus*)

History:
On March 29, 2022, a crow die-off occurred in a public garden in Sapporo, Hokkaido, Japan. Based on RT–qPCR and subsequent gene sequencing analyses, carcasses collected on March 29 and May 18, 2022, were confirmed to be infected with highly pathogenic avian influenza virus (HPAIV). On the same day as the die-off, a diseased raccoon dog was also noticed by the garden workers. Three days thereafter, the raccoon dog showed severe clinical signs of depression and blindness. It was captured for treatment but was considered to be at a humane endpoint from the veterinary viewpoint; thus, it was euthanized via isoflurane inhalation. The raccoon dog was subjected to postmortem examination.

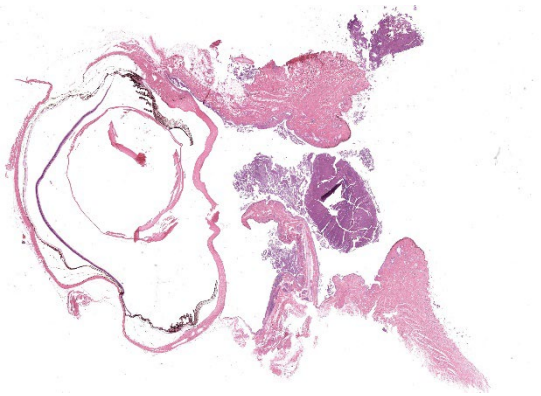

Figure 2-1. Globe and palpebra, raccoon dog. Aggregates of inflammatory debris are present within the palpebral fissure and beneath the eyelid. (HE, 7X)

Gross Pathology:
The raccoon dog was severely emaciated and moderately dehydrated. Severe bilateral conjunctivitis with eye discharge was noted, and the lenses were mildly clouded. Nematodes were detected in the stomach. The kidneys were discolored.

Laboratory Results:
HPAIV genomes of the H5 subtype were detected and the virus was isolated from the 10% homogenates of the brain, trachea, and lung of the raccoon dog.[2]

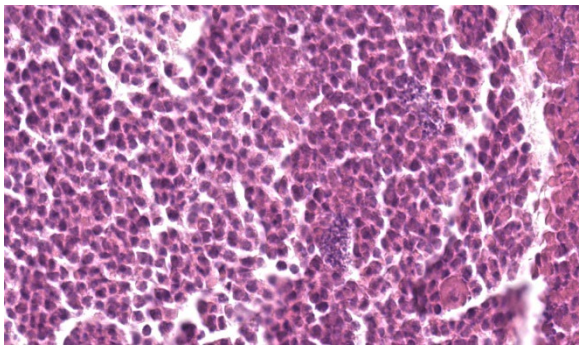

Figure 2-2. Palpebral fissure, raccoon dog. High magnification of the exudate within the palpebral fissure which is composed of viable and necrotic neutrophils, debris-laden macrophages, abundant cellular debris, and entrapped bacterial colonies. (HE, 1100X)

Microscopic Description:
Numerous degenerated and necrotic neutrophils and bacterial colonies are evident in the palpebral fissure. There is a mild infiltration of lymphocytes and neutrophils in the lamina propria of the palpebral and bulbar conjunctiva of the upper eyelid. A moderate to severe lymphoplasmacytic and mild neutrophilic infiltration with mild fibrosis is observed in the lamina propria of the third and lower eyelid. Desquamation of conjunctival epithelial cells is sometimes seen.

Contributor's Morphologic Diagnosis:
Eye (left): Conjunctivitis, diffuse, chronic, suppurative, severe

Contributor's Comment:
Immunohistochemistry using anti-influenza virus NP (nucleoprotein) monoclonal antibody (clone 183/5), detected viral antigens in columnar epithelia lining the bulbar and palpebral conjunctiva, most notably of the third eyelid.[3] Moreover, viral antigens were detected in the superficial glands under the conjunctiva of the third eyelid.[3]

This raccoon dog was found emaciated in the same park on the same day that the HPAIV-infected crow was found dead. Raccoon dogs show greater dependency on fruits, plant seeds, and insects, although they also consume animal resources during spring.[1] That stated, garden workers did not observe this animal scavenging crow carcasses. Presumably, this raccoon dog was in in close contact with crow carcasses even if it did not ingest them.

In tissues other than conjunctiva, viral antigens were detected only in the tracheal ciliated epithelium and tracheal glands.[3] Titers of infectious viruses found in the brain, lung and trachea homogenates were close to the limit of detection,[3] which is likely due to clearance of the virus by an immune response. Visual impairment is usually critical for wildlife animals. It was speculated that although the raccoon dog survived the acute phase of HPAIV infection, visual impairment caused by the secondary bacterial infection resulted in malnutrition and dehydration.

Contributing Institution:
Laboratory of Comparative Pathology
Department of Clinical Sciences
Faculty of Veterinary Medicine
Hokkaido University
Kita18, Nishi 9, Kita-ku, Sapporo 060-0818, JAPAN
https://www.vetmed.hokudai.ac.jp/organization/comp-pathol/e/index.html

JPC Diagnosis:

Conjunctiva: Conjunctivitis, neutrophilic and lymphoplasmacytic, chronic-active, diffuse, marked.

JPC Comment:
This second case has an interesting backstory that comes full circle to current events and the ongoing spread of H5N1 HPAI clade 2.3.4.4b viruses worldwide. We previously

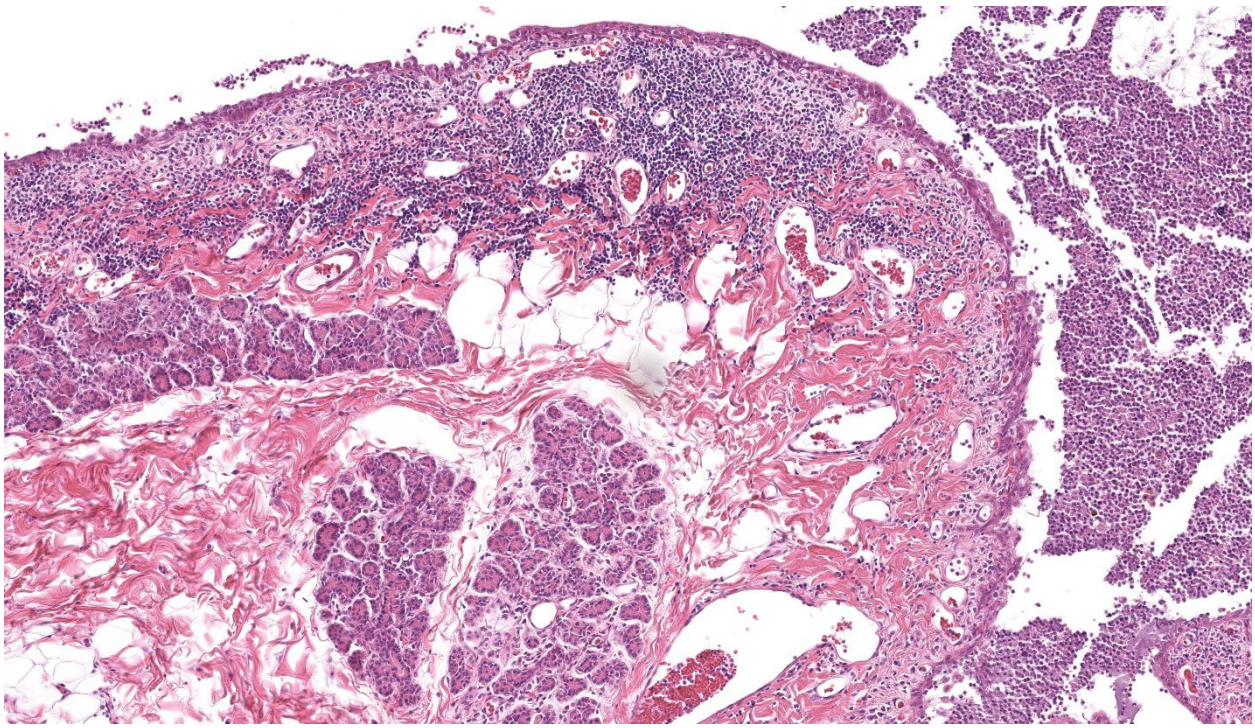

Figure 2-3. Eyelid conjunctiva. The conjunctival epithelium is hyperplastic and multifocally eroded. The subconjunctival tissue is infiltrated by large numbers of neutrophils, lymphocytes and plasma cells, which also expand the interstitial collagen between acini of the lacrimal gland. (HE, 180X)

touched on avian influenza in the context of an experimental case in a pig (Case 3, Conference 14, 2024-2025). Although we discussed the role of viral shedding into milk and zoonotic potential therein, there is still plenty more left to say on this topic.

The slide description for this case is not overly complicated, though conference participants did not immediately offer HPAI as a presumptive cause for the disruption of the conjunctival epithelium and subsequent bacterial infection in this animal. Conjunctivitis is underappreciated as a clinical sign of HPAI, though recent human cases acquired from dairy or poultry workers[2,7] have shown that this may be the only overt sign of disease. Similar to the tanuki in this case, workers exposed to HPAI may only be exposed through the conjunctiva because of mask/glove wear or occupational factors such as the proximity of the eyeline of milking parlor workers to the udders of the cows being milked. In comparison to the red fox that scavenged the carcass and developed systemic viral infection[3], this animal had evidence of chronic infection and a host adaptive immune response – this may reflect a lower viral load and impact of the route of entry. The role of α2,3 sialic acid receptors on conjunctival epithelium and zoonotic transmission of avian influenza viruses has previously been established and likely played a role in the present case.[3,4]

Similar to the fox's outcome in the present case[3], domestic cats have fallen ill or died after consumption of raw pet food diets and/or exposure to raw milk contaminated with HPAI.[5] Systemic entry of HPAIV has been associated with endothelial cell targeting and vasculitis, a feature which is noticeably absent in this tanuki. Other classic manifestations of HPAI (in cats and beyond) include

pancreatic necrosis, encephalitis, myocarditis, and adrenal necrosis.[6,8]

Finally, the contributor gave us a final puzzle to ponder for this case. As the animal was submitted as an 'Ezo' raccoon dog, we explored this aspect further. Accordingly, Ezo is borrowed from the Ainu language (an indigenous people from Northern Japan) and refers to the northern part of Meiji-era Japan, particularly Hokkaido, but also Sakhalin and the Kuril Islands.[9] In modern usage, the term has largely disappeared, but is used to refer to several species native to northern Japan such as the Ezo fox (北狐), Ezo deer (エゾシカ) and Ezo tanuki (エゾタヌキ). Additionally, there is not a consensus on the taxonomy, with *Nyctereutes procyonoides albus* and *Nyctereutes viverrinus* both being used to refer to the same species native to Japan. As the contributor of this case is from Hokkaido and refers to the animal as a tanuki,[3] we conclude that this is a native Japanese raccoon dog and not a related species that has been widely distributed across Asia and Europe.

References:

1. Akihito TS, Teduka M, Kawada S. Long-term Trends in Food Habits of the Raccoon Dog, Nyctereutes viverrinus, in the Imperial Palace, Tokyo. *Bull. Natl. Mus. Nat. Sci*., Ser. A. 2016;42(3):143–161.
2. Drehoff CC, White EB, Frutos AM, et al. Cluster of Influenza A(H5) Cases Associated with Poultry Exposure at Two Facilities - Colorado, July 2024. *MMWR Morb Mortal Wkly Rep*. 2024 Aug 29;73(34):734-739.
3. Hiono T, Kobayashi D, Kobayashi A, et al. Virological, pathological, and glycovirological investigations of an Ezo red fox and a tanuki naturally infected with H5N1 high pathogenicity avian influenza viruses in Hokkaido, Japan. *Virology*. 2023;578:35-44
4. Olofsson S, Kumlin U, Dimock K, Arnberg N. Avian influenza and sialic acid receptors: more than meets the eye? *Lancet Infect Dis*. 2005 Mar;5(3):184-8.
5. Schnirring L. H5N1 confirmed in more cats as probe into raw pet food widens. University of Minnesota Center for Infectious Disease Research and Policy (CIDRAP). 2025 Jan 14; https://www.cidrap.umn.edu/avian-influenza-bird-flu/h5n1-confirmed-more-cats-probe-raw-pet-food-widens.
6. Soda K, Tomioka Y, Usui T, et al. Susceptibility of herons (family: Ardeidae) to clade 2.3.2.1 H5N1 subtype high pathogenicity avian influenza virus. *Avian Pathol*. 2022 Apr;51(2):146-153.
7. Uyeki TM, Milton S, Abdul Hamid C, et al. Highly Pathogenic Avian Influenza A(H5N1) Virus Infection in a Dairy Farm Worker. *N Engl J Med*. 2024 Jun 6;390(21):2028-2029.
8. Wünschmann A, Franzen-Klein D, Torchetti M, Confeld M, Carstensen M, Hall V. Lesions and viral antigen distribution in bald eagles, red-tailed hawks, and great horned owls naturally infected with H5N1 clade 2.3.4.4b highly pathogenic avian influenza virus. *Vet Pathol*. 2024 May;61(3):410-420.
9. Tanoshii Japanese. Ezo. https://www.tanoshiijapanese.com/dictionary.

CASE III:

Signalment:
Juvenile, female Angus cow, bovine (*Bos taurus*)

History:
This cow was one of 45 presenting with cutaneous lumps when mustered from a herd of 95 animals. Rectal temperatures ranged from 40-41ºC and some of the affected cows appeared sick. Some cows were panting with

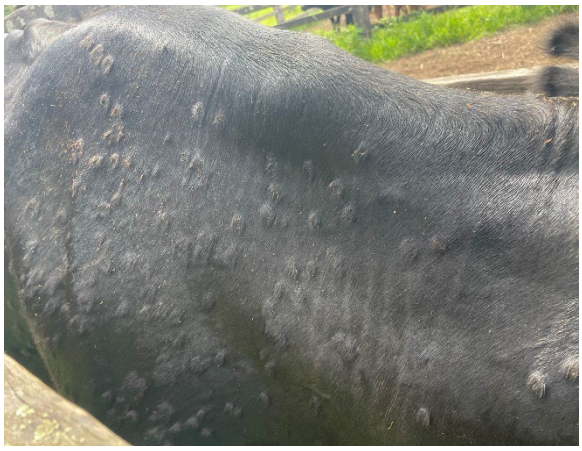

Figure 3-1. Haired skin, ox. Photograph from one of the affected cows in the herd. Skin nodules were raised, non-ulcerated and ranged from 10-30mm diameter and were frequently over the neck and brisket. (*Photo courtesy of:* Dr. Phillip Carter, Local Land Services, New South Wales)

increased lung sounds. The mucous membranes were pink. There was no evidence of typical photosensitization lesions in predisposed locations.

Gross Pathology:
Nodules were distributed over the neck, brisket, thorax and to a lesser extent abdomen and forelimbs. Nodules ranged from 10-30mm diameter and were not ulcerated, although the surface of some could be scratched off.

Laboratory Results:
A Pan-Herpesvirus nested PCR was performed, and the product was sent for Sanger sequencing. A BLAST query of the product sequence found it was 100% identical to Bovine alphaherpesvirus 2 [MT862164] 181 nt partial sequence. A ruminant biochemistry panel found elevation in GLDH 96 U/L (0-30 U/L), mild hyperglobulinaemia 48.4 g/L (30.0-45.0 g/L) and mild elevation in serum hemoglobin 0.25 g/dL (0.00-0.20 g/dL). A Capripoxvirus TaqMan assay on the EDTA blood and a skin scab was negative, and a Capripox double antigen multispecies ELISA performed on the serum sample was negative.

Microscopic Description:
Haired skin (x3): Within the sections of haired skin, multifocally within the epidermis, there are hypereosinophilic necrotic keratinocytes, numerous small expansions containing eosinophilic fluid (vesicles) and necrotic cell debris and degenerate neutrophils, sometimes forming small aggregates (micropustules). Multifocally, epithelial cells within the stratum basale, stratum spinosum and stratum granulosum are sloughed, replaced with clumps of multinucleated epithelial cells with hypereosinophilic cytoplasm (syncytia). Moderate numbers of epithelial cells and syncytia within the surface epithelium, and occasionally within epithelium lining hair follicles, contain 1-6µm diameter intranuclear eosinophilic inclusion bodies with margination of chromatin. Multifocally, keratinocytes are swollen with clearing of cytoplasm (ballooning degeneration). There is mild, multifocal orthokeratotic hyperkeratosis, with mild to moderate extravasated erythrocytes adjacent to the epidermal surface (hemorrhage). Throughout the superficial and

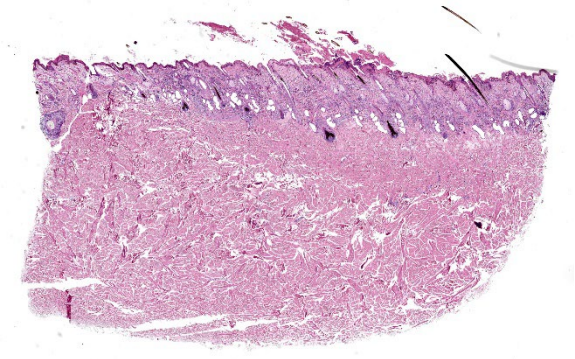

Figure 3-2. Haired skin, ox. One section of haired skin is submitted for examination. There is diffuse epidermal hyperplasia, foal hyperkeratosis and pustule formation, and a diffuse band of hypercellularity within the superficial dermis. (HE, 7X)

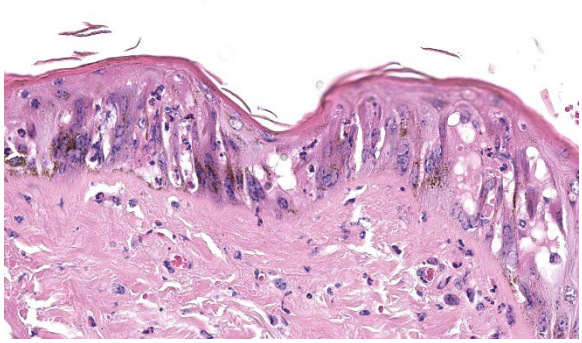

Figure 3-3. Haired skin, ox. There are numerous viral cytopathic changes within the epidermis including intra- and intercytoplasmic edema with vesicle formation, syncytia formation, and intranuclear and intracytoplasmic viral inclusions. (HE, 705X)

deep dermis, there are multifocal, moderate infiltrates of neutrophils, lymphocytes, plasma cells, eosinophils and macrophages associated with cell debris, and multifocal mild to moderate separation of dermal collagen fibres with clear space and/or eosinophilic fluid (edema). Occasionally sebaceous glands are surrounded and infiltrated by neutrophils and apocrine glands are dilated. Few lymphatic vessels in the deep dermis are dilated. Within the dermis of one section, adjacent to the cut margin, there is a focal aggregate of refractile material, surrounded by eosinophilic necrotic material, and subsequently surrounded by a moderate margin of leukocytes with squash artefact.

Contributor's Morphologic Diagnosis:
Haired skin, dermatitis, necrosuppurative and, lymphoplasmacytic multifocal to widespread, chronic-active, with edema, syncytial cells, pustules, vesicles and intranuclear epithelial eosinophilic viral inclusion bodies, *Bos taurus.*

Contributor's Comment:
Infection with Bovine Herpesvirus 2 (BoHV-2) in cattle can cause two distinct clinical conditions: one is an acute onset, mild generalized skin infection called Pseudo Lumpy Skin Disease (PLSD) which manifests as cutaneous nodules which develop a central depression; the second is Bovine Herpesvirus Mammillitis (BHM), a localized ulcerative condition affecting the teats and udder of cattle. The disease is found in many parts of the world and is likely transmitted by biting insects or mechanically by equipment used on farms. The gross appearance of the generalized skin lesions can closely resemble Lumpy Skin Disease, which has trade implications in many countries.[21]

Bovine herpesvirus 2 (BoHV-2) is an enveloped double stranded DNA virus approximately 150-200nm in size, belonging to the family Orthoherpesviridae, subfamily Alphaherpesvirinae, genus simplexvirus**.**

Bovine herpesvirus 2 infection was first identified in Southern and Eastern Africa. Since its discovery in the 1950's, it has been reported almost globally with case reports from Europe, Japan, Australia, Brazil, the United States and Israel.[2,3,8–10,13,16]

In the wild, BoHV-2 infects cattle, wild ruminants and pseudo-ruminants (hippopotamus).[13] Sheep have been experimentally infected with BoHV-2 producing clinical dis-

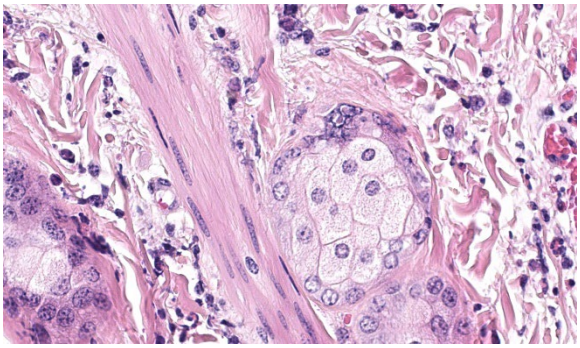

Figure 3-4. Haired skin, ox. Viral inclusions and syncytia are present within reserve cells of sebaceous glands. (HE, 847X)

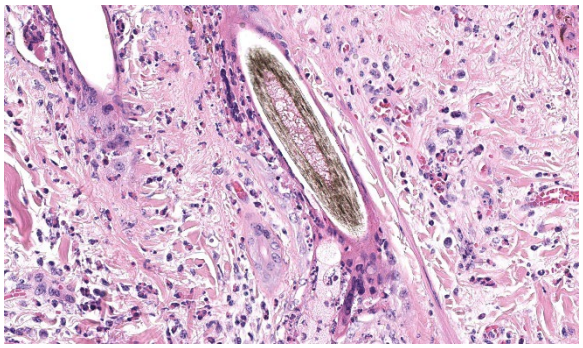

Figure 3-5. Haired skin, ox. Viral inclusions and syncytia are present within follicular epithelium. (HE, 531X)

ease similar to Bovine Herpesvirus Mammillitis.[17] Rabbits, guinea pigs and mice have also been experimentally infected with BoHV-2.[8]

Transmission of BoHV-2 most likely occurs via intradermal injection of the virus by biting insects, or via contaminated equipment coming into contact with wounds and cuts. Biting flies have been demonstrated to be able to transmit the infection between cell cultures in the lab, and the distribution and seasonality of outbreaks of Pseudo Lumpy Skin Disease are thought to be related to the distribution and peaks in biting insect activity.[6,9,12] Milking equipment is suspected of being able to transmit the virus within milking herds if clinically affected cattle are present.[5,10]

Serological surveys indicate that circulation of BoHV-2 in cattle can occur without any episodes of clinical disease suggesting most infections may be subclinical.[8,9,15]

In experiments where BoHV-2 was intradermally inoculated into the flank of cattle, a discrete raised swelling was observed at the injection site by day 3 post inoculation. Generalized discrete swellings appeared over the head, neck and dorsal body by day 6 which developed crusts which gradually lifted over the course of 3 weeks to reveal greyish-white areas of skin with reduced numbers of hairs (alopecia). Lymph node enlargement was observed by day 5 and persisted to day 10 post inoculation.[16]

In the field, the incubation period of BoHV-2 is considered to be around 1-2 weeks, with skin lesions resolving 2-4 weeks after first appearing. Neutralizing antibodies appear 7-14 days after initial exposure.[16,18] Outbreaks can occur seasonally or sporadically depending on the activity of biting insects and the presence of naive hosts.[11,19]

Post infection, like other herpesviruses, BoHV-2 becomes latent with the virus likely retreating to the neuronal tissue such as the trigeminal ganglion and possibly lymphoid tissue where it may lay dormant until infection is reactivated during periods of stress.[3,17]

Generalized infection with BoHV-2 induces Pseudo Lumpy Skin Disease, which is characterized by:[1,4,16]

- Circumscribed cutaneous nodules over the body, frequently on the head, neck, shoulders, back and perineum.
- Around 4-6 days after the appearance of gross lesions, the cutaneous lesions begin to crust over. The crusts eventually fall off leaving areas of alopecia.
- Lesions disappear when the hair regrows.
- Lymphadenitis may be observed during early stages of infection.
- Animals make a full recovery without treatment.

Localized infection with BoHV-2 of the udder and teats is called Bovine Herpesvirus Mammillitis, and is characterized by:[11,20]

- Variable sized tender edematous swellings on the udder or teats.
- Vesicles may appear on affected areas
- The overlying skin then ulcerates and becomes painful, taking 3-10 weeks to heal

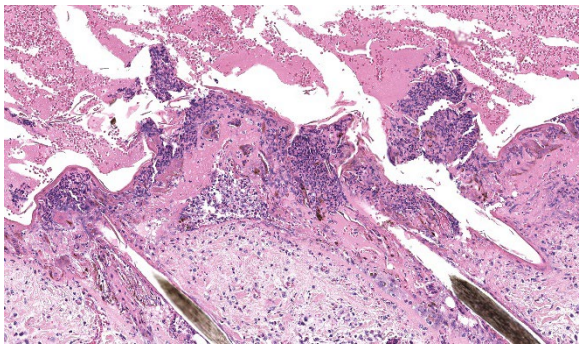

Figure 3-6. Haired skin, ox. There is multifocal full-thickness epidermal necrosis and pustule formation. (HE, 261X)

Histopathological changes of BoHV-2 infection are characterized by the formation of epithelial syncytia initially within the stratum basale and inner stratum spinosum with prominent intranuclear eosinophilic inclusion bodies.[11] Intranuclear inclusions are classified as Cowdry type A inclusions and have central eosinophilic or amphophilic deposits surrounded by a clear halo and the nuclear chromatin is pushed to the margin of the nucleus.[19] Intranuclear inclusions are most numerous after the appearance of the gross nodules but before the appearance of crusts (around 4-6 days later),[1,11] which coincides approximately with the time when virus can be isolated or detected by PCR (see below). When the lesions crust over, the epithelium becomes necrotic and infiltrated by large numbers of neutrophils. Loss of the necrotic epithelium results in an ulcer which becomes covered with haemorrhage, fibrinous exudate and numerous degenerate neutrophils. Deeper in the dermis, there is edema and a mononuclear infiltrate. As the lesion heals, there is fibrosis in the superficial dermis with perivascular infiltrates of mononuclear cells.[11]

The following assays have been reported in the literature to support the diagnosis of BoHV-2 infection.

Test	Required Samples	Notes
PCR[1,12,19]	Fresh skin lesions	Most likely to yield detectable virus DNA up to 8 days post infection or before cutaneous lesions crust over or ulcerate
Cytology[11]	Early skin lesions (<5 days after initial appearance)	Presence of syncytia with intranuclear inclusions
Serology - ELISA[15]	Serum	
Serology – Serum neutralization[9,18]	Serum	Antibodies detected as early as 10 days post inoculation or about 5-7 days after appearance of cutaneous lesions
Serology – Immunofluorescent antibody test (IFAT)[10]	Serum	
Negative staining electron microscopy[19]	Fresh skin lesions	Herpesvirus particles may be seen
Virus culture[6,9,10,16,18]	Blood, Fresh skin lesions up to around day 6-7 post infection	Vero cells Calf kidney cells Fetal bovine muscle cells Madin Darby Bovine Kidney (MDBK)

The following conditions should be considered as potential differentials for Bovine Herpesvirus-2 infection based on their clinical appearance.[4,11,20]

Disease	Clinical Presentation	Tests to diagnose/ differentiate	Key differentiating histological features
Viral			
Early-stage Lumpy Skin Disease (Capripoxvirus)	Firm circumscribed cutaneous nodules which develop central areas of necrosis and scarring	Capripox PCR, biopsy + histopathology, Electron microscopy demonstrating pox virus particles	Epidermal vacuolar swelling with intracytoplasmic inclusions. Vasculitis
Bovine Papillomavirus	Papillomas or warts of varying size on body. Mostly frequently seen in younger cattle	Biopsy + histopathology, PCR of skin lesions	Unencapsulated, proliferative cutaneous neoplasm accompanied by basal cell hyperplasia, acanthosis and hyperkeratosis
Bovine papular stomatitis (Parapoxvirus)	Raised red papules, erosions or ulcers around muzzle and nose, occasionally elsewhere on the body	Electron microscopy of tissue, virus culture, biopsy + histopathology, ELISA/Agar gel precipitation tests to look for antibodies	Epidermal vacuolar swelling with intracytoplasmic inclusions, epidermal proliferation
Pseudocowpox (Parapoxvirus)	Raised red sores, scabs or vesicles on teats, thighs or perineum	PCR on skin lesions, scabs or blood, biopsy + histopathology.	Epidermal vacuolar swelling with intracytoplasmic inclusions, epidermal proliferation
Cowpox (Orthopoxvirus)	Papules or ulcers on the teat or udder	PCR of skin lesions, electron microscopy of scabs demonstrating pox virus particles[14], biopsy + histopathology	Epidermal vacuolar swelling with intracytoplasmic inclusions, focal epidermal hyperplasia.
BVDV dermatitis	Patchy hyperkeratosis	Bovine Viral Diarrhea	

	around neck, shoulder and perineum	Virus Antigen ELISA or PCR on ear notch, blood, hair or visceral organs	
Bovine Herpesvirus 4	Vesicles, pustules and ulcers on udder. Teats are usually not involved	PCR on skin lesions, serological testing, biopsy + histopathology	Intraepithelial pustular dermatitis
Bacterial			
Dermatophilosis (*Dermatophilus congolensis*)	Papules with crusts entrapped in hair and areas of alopecia often over the dorsal aspect of head, neck and body	Bacterial cultures, cytology of crusts, biopsy + histopathology	Multiple parallel rows of cocci, trapped within alternating layers of hyperkeratosis and serous fluid and degenerate neutrophils. Purulent folliculitis
Cutaneous tuberculosis (*Mycobacterium bovis*)	Single or multiple nodules, abscesses or ulcers	PCR, mycobacterial culture, biopsy + histopathology	Pyogranulomatous dermatitis with central caseous necrosis with acid fast bacilli present.
Fungal			
Dermatophytosis (Ringworm, *Trichophyton verrucosum*)	Expanding circular hairless lesions mostly on head and neck. May appear red and moist to scaly and grey.	Dermatophyte cultures, biopsy + histopathology, PCR	Fungal hyphae clustering within hair shafts and arthrospores around the outside of hairs.
Parasites			
Mites (multiple species)	Nodules, alopecia and crusts which may be itchy	Superficial or deep skin scrapings	

Onchocercosis	Cutaneous nodules over brisket, abdomen and udder	Biopsy + histopathology	Presence of microfilaria, surrounded by eosinophilic inflammation
Besnoitiosis (*Besnoitia sp.*)	Alopecia, scaling and thickening of skin over neck ,shoulders and rump	biopsy + histopathology, PCR, serology	Presence of protozoal tissue cysts
Hypoderma sp. (warbles)	Firm raised nodules in the skin frequently along the back and shoulders	Clinical examination and presence of breathing holes Serological tests	
Neoplasia			
Cutaneous Lymphoma	Multifocal subcutaneous/intracutaneous nodules, often accompanied by alopecia, lymphadenopathy	biopsy + histopathology, haematology may reveal lymphocytosis. May arise sporadically and not necessarily be associated with bovine leukosis virus infection	Sheets of neoplastic lymphocytes.
Mast cell tumor	Mulltifocal cutaneous or subcutaneous nodules over body +/- alopecia +/- pigmented +/- ulceration	biopsy + histopathology	Sheets of neoplastic mast cells often accompanied by numerous eosinophils
Other			
Photosensitization	Alopecia, erythema and blistering of non-pigmented skin	History – exposure to toxic plants, drug administration, biochemistry – liver function, biopsy +	Coagulative necrosis of epidermis, dermal edema, vascular necrosis

		histopathology	
Skin allergies/urticaria	Haired wheals +/- crusts anywhere on the body, angioedema	History of recent drug administration, insect or plant exposure, response to glucocorticoid administration, biopsy + histopathology	Dermal edema, perivascular infiltrates of granulocytes, mast cells and lymphocytes inconsistently present in upper to mid dermis.

Contributing Institution:
Elizabeth Macarthur Agricultural Institute, Department of Primary Industries and Regional Development

JPC Diagnosis:
Haired skin: Dermatitis, necrotizing, subacute, diffuse, severe, with epithelial viral syncytia, intranuclear viral inclusions, corneal pustules, mixed dermal infiltrates, and edema.

JPC Comment:
The contributor provides an excellent section to accompany an thorough writeup on the topic. The slide has generous viral inclusions and syncytia along with raised vesicles to establish an etiological diagnosis. Conference participants did touch on the nature of intracellular and intercellular edema in this case – the lack of overt cellular swelling and intracytoplasmic inclusions lowered suspicion for a poxviral etiology.

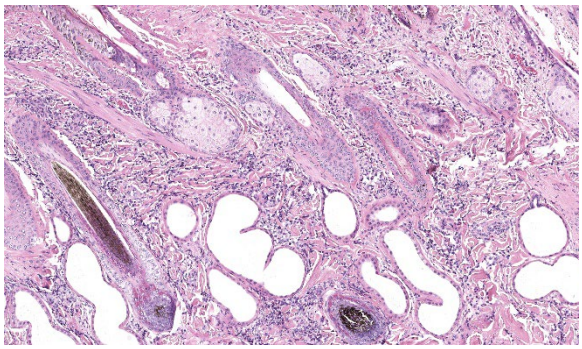

Figure 3-7. Haired skin, ox. There is marked mixed dermal inflammation, dilation of apocrine glands, and thickened and tortuous dermal arterioles. (HE, 179X)

One ancillary finding in section was a focal granuloma centered on foreign material (possibly plant material). We speculated that this might be secondary to necrosis of the overlying epithelium and entry into the dermis, though the adjacent portions of skin lack significant viral changes. This lesion is at the edge of the section and is only on one of the three sections of skin provided which limits further interpretation of this incidental observation.

References:

1. Amaral B, Dos Santos Jardim J, Cargnelutti J, Martins M, Weiblen R, Flores E. Pathogenesis of Bovine alphaherpesvirus 2 in calves following different routes of inoculation. *Pesqui Veterinária Bras*. 2020;40:360–367.
2. Brenner J, Sharir B, Yadin H, Perl S, Stram Y. Herpesvirus type 2 in biopsy of a cow with possible pseudo-lumpy-skin disease. *Vet Rec*. 2009;165(18):539–540.
3. Campos FS, Franco AC, Oliveira MT, et al. Detection of bovine herpesvirus 2 and bovine herpesvirus 4 DNA in trigeminal ganglia of naturally infected cattle by polymerase chain reaction. *Vet Microbiol*.

2014;171(1):182–188.
4. Department of Agriculture, Fisheries and Forestry. Differential diagnoses for lumpy skin disease. Australian Government 2023:
5. Gibbs EPJ, Johnson RH, Osborne AD. Experimental Studies of the Epidemiology of Bovine Herpes Mammillitis. *Res Vet Sci*. 1973;14(2):139–144.
6. Gibbs EPJ, Jonnson RH, Gatehouse AG. A Laboratory Technique for Studying the Mechanical Transmission of Bovine Herpes Mammillitis Virus by the Stable Fly (Stomoxys calcitrans L.). *Res Vet Sci*. 1973;14(2):145–149.
7. Hulo C, de Castro E, Masson P, et al. ViralZone: a knowledge resource to understand virus diversity. *Nucleic Acids Res*. 2011;39(Database issue):D576-582.
8. Huygelen C, Thienpont D, Dekeyser PJ, Vandervelden M. Allerton Virus, a Cytopathogenic Agent Associated with Lumpy Skin Disease. *Zentralblatt Für Veterinärmedizin*. 1960;7(8):754–760.
9. Imai K, Ishihara R, Nishimori T. First demonstration of bovine herpesvirus 2 infection among cattle by neutralization test in Japan. *J Vet Med Sci*. 2005;67(3):317–320.
10. Lanave G, Larocca V, Losurdo M, et al. Isolation and characterization of bovine alphaherpesvirus 2 strain from an outbreak of bovine herpetic mammillitis in a dairy farm. *BMC Vet Res*. 2020;16(1):103.
11. Mauldin EA, Peters-Kennedy J. Chapter 6 - Integumentary System. In: Maxie MG, ed. *Jubb, Kennedy & Palmer's Pathology of Domestic Animals: Volume 1 (Sixth Edition)*. W.B. Saunders 2016:509-736.e1.
12. d'Offay JM, Floyd JG, Eberle R, et al. Use of a polymerase chain reaction assay to detect bovine herpesvirus type 2 DNA in skin lesions from cattle suspected to have pseudo-lumpy skin disease. *J Am Vet Med Assoc*. 2003;222(10):1404–1407, 1366–1367.
13. Plowright W, Jessett DM. Investigations of Allerton-type herpes virus infection in East African game animals and cattle. *J Hyg (Lond)*. 2009/05/15 ed. 1971;69(2):209–222.
14. Shivanna V, Cino-Ozuna AG, Heskett C, Marthaler DG, Ganta C. Pseudocowpox virus infection in an American bison (Bison bison). *BMC Vet Res*. 2020;16(1):241.
15. Singer S, Hoffmann B, Hafner-Marx A, et al. Bovine Alphaherpesvirus 2 infections in Bavaria: an analysis of the current situation - several years after eradicating Bovine Alphaherpesvirus 1. *BMC Vet Res*. 2020;16(1):149.
16. St George TD, Uren MF, Melville LF. A generalised infection of cattle with bovine herpesvirus 2. *Aust Vet J*. 1980;56(1):47–48.
17. Torres FD, Almeida SR, Silva MS, Weiblen R, Flores EF. Distribution of latent bovine herpesvirus 2 DNA in tissues of experimentally infected sheep. *Res Vet Sci*. 2009;87(1):161–166.
18. Turner AJ, Kovesdy L, Morgan IR. Isolation and characterisation of bovine herpesvirus mammillitis virus and its pathogenicity for cattle. *Aust Vet J*. 1976;52(4):166–169.
19. Watanabe TTN, Moeller RB, Crossley BM, Blanchard PC. Outbreaks of bovine herpesvirus 2 infections in calves causing ear and facial skin lesions. *J Vet Diagn Invest*. 2017;29(5):686–690.
20. White SD, Théon AP, Angelos JA, Makhdoomi MM. Chapter 40 - Diseases of the Skin. In: Smith BP, Van Metre DC, Pusterla N, eds. *Large Animal Internal Medicine (Sixth Edition)*. Mosby 2020:1316-1351.e11.
21. World Organisation for Animal Health. Infection with lumpy skin disease virus. In: *Terrestrial Animal Health Code*.

World Organisation for Animal Health (OIE) 2024:

CASE IV:

Signalment:
8 week old, female intact, C.B-17 *scid* mouse (*Mus musculus*).

History:
This mouse was part of research project to study the role *B. burgdorferi* virulence factors in the pathogenesis of Lyme Borreliosis. The mouse was inoculated on the lumbosacral region via SQ with *Borrelia burgdorferi* B31- A3 strain and was euthanized 4 weeks post-challenge.

Gross Pathology:
Bilaterally, the tibotarsal joints were markedly thickened and swollen on the cranial aspect.

Laboratory Results:
BSK-II culture media was positive for *B. burgdorferi*. Spirochetes were isolated from a section of the tibiotarsal joint. White blood cell counts demonstrated a neutrophilia (5.57, ref 0.43 – 3.58 K/uL). Spirochetes were demonstrated in areas of tenosynovitis by immunohistochemistry and Warthin-Starry stain in the tibiotarsal joints.

Microscopic Description:
Tibiotarsal joint. Arising from antero-distal tibial metaphysis to the antero-proximal aspect of the tarsal bones is a well-demarcated, densely cellular, thickened and inflamed synovium, regionally admixed with an irregular trabecula of woven bone. The synovium is markedly hyperplastic by numerous, variably sized, spindle to spindloid synovial cells closely packed to each other and is lined by a discontinuous, single layer of plump synoviocytes. The synovium is diffusely infiltrated by large numbers of neutrophils and moderate

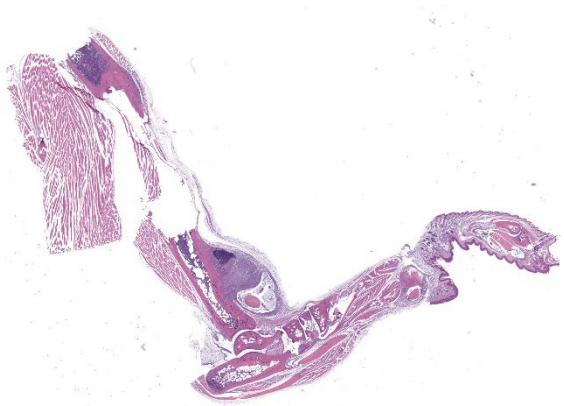

Figure 4-1. Leg, SCID mouse. A section of hind leg is submitted for examination. At subgross magnification, there is marked expansion of the tibiotarsal joint. (HE, 7X)

numbers of macrophages. The synovial space and tendon sheaths are infiltrated by moderate numbers of neutrophils and fewer macrophages mixed with eosinophilic proteinaceous fluid, fibrin, sloughed cells, necrotic cells, and karyorrhectic debris. The periosteum along antero-distal tibial metaphysis and epiphysis is expanded by an irregular intertwined trabecula of woven bone that is incompletely mineralized (periosteal remodeling) and contains numerous osteocytes. The immature trabecula is lined by osteoblasts, entraps mesenchymal stromal cells, and is regionally bounded by organized island of cartilage undergoing endochondral ossification (bone formation). The edges of the woven bone are irregular and scalloped and often lined by osteoblasts and fewer osteoclasts within Howship's lacunae (remodeling). Within the inflamed synovium a focal subperiosteal trabecula, arranged perpendicularly to zones of bone remodeling, is composed of woven bone at different stages of mineralization. The synovium and adjacent tendon sheaths in the remaining proximal tarsal bones and plantar aspect of the tibiotarsal joint is mildly hyperplastic and infiltrated by low numbers of macrophages. In these areas synovial spaces contain proteinaceous fluid mixed with individual sloughed synovial cells and rare karyorrhectic debris.

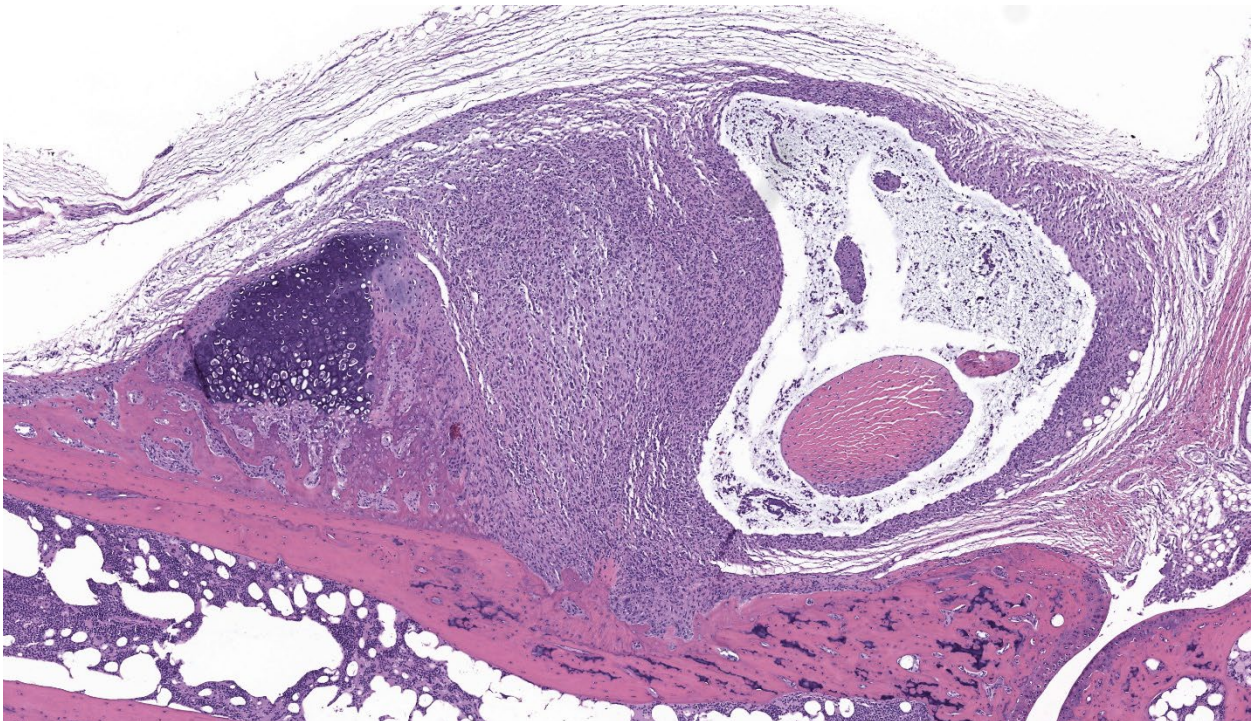

Figure 4-2. Tibiotarsal joint, SCID mouse. The tendon sheath is markedly expanded up to 1mm and the interface between it and the underlying synovium is effaced by abundant granulation tissue. Granulation tissue infiltrates the lamellar bone of the distal tibia. Dorsal to the tibiotarsal joint, there is marked periosteal new bone growth with a focal area of mature cartilage. (HE, 75X)

Contributor's Morphologic Diagnosis:
Tibiotarsal joint: Tenosynovitis**,** neutrophilic and histiocytic, with synovial hyperplasia and hypertorphy, periosteal bone formation and remodeling, regional, marked, chronic.

Contributor's Comment:
The C.B-17 *scid* (SCID) mouse presented in this submission was part of a study to determine the pathogenicity and tropism of *Borrelia burgdorferi* strains deficient in different virulence factors. The mouse was part of a control group of SCID mice that were inoculated with a high dose of *B. burgdorferi* B31-A3 (wild-type) strain. C.B-17 *scid* (SCID) mice are *homozygous* for the *Prkdc*^{scid} mutation resulting in severe combined immunodeficiency.[7] This mouse strain lacks functional lymphocytes (both T and B cells) because of impaired VDJ rearrangement.[7] SCID mice exhibited the following features: marked lymphopenia, agammaglobulinemia, and high susceptibility to opportunistic infections.[7,11]

The use of laboratory mice has provided valuable insights into the immune response and pathogenesis of Lyme arthritis and carditis. Mice infected with *Borrelia burgdorferi* (*Bb*) can also develop myositis, arteritis/vasculitis, and peripheral neuritis, which parallel with lesions seen in Lyme disease patients.[1,3,4] There are several factors that should be considered when evaluating phenotypes in this model. For example, disease severity in laboratory mice is influenced by genotype, immune status, age of the mice, *Bb* strain and passage history of the strain, infectious dose, and route of inoculation.[2,4,9] It is well-accepted that inbred mouse strains are equally

susceptible to *Bb* infection, but the susceptibility of arthritis is dependent on the mouse genotype.[3]

The C3H/HeN and C3H/HeJ mice are often used to study histopathological changes in the joints as these mouse strains develop moderate to severe subacute tenosynovitis in the tibiotarsal joints.[3,4] *Bb* reaches the tibiotarsal joint after 2 weeks of intradermal or subcutaneous inoculation of spirochetes.[4] At 4 weeks of infection, the inflammation in synovium, tendon sheaths, and periarticular connective tissue is predominantly composed by neutrophils mixed with moderate numbers of macrophages, fibrinous exudate in joint lumen, and hyperplasia and hypertrophy of the synovium surrounding the tibiotarsal joints.[4] BALB/c mice develop mild to moderate tenosynovitis and C57BL/6 mice develop mild tenosynovitis following infection with *Bb*.[4,12] In contrast, SCID mice develop more severe tenosynovitis than immunocompetent mouse strains as SCID mice exhibit higher bacterial loads in the tibiotarsal joints and develop persistent infections in tissues.[4] The lesions seen in the tibiotarsal joints of SCID mice infected with *Bb* are characterized by marked hyperplasia and hypertrophy of synoviocytes with multifocal moderate to marked neutrophilic to histiocytic inflammation in synovium, ligaments, and tendon sheaths (e.g., tibiotarsal extensor tendon), fibrin and proteinaceous exudate.[3,4] As shown in this case the lesions are commonly noted at 4 weeks of infection but can persist for 8 weeks post-inoculation when mice SCID mice are inoculated with high doses of *Bb*. Spirochetes are readily visible by silver stains and/or immunohistochemistry, which are often observed within the proliferating synovium and associated with neutrophils and macrophages. The distal tibia in SCID mice often exhibits areas of periosteal remodeling and endochondral ossification with new bone formation.[3,4] Occasionally, severe lesions in SCID mice can develop progressive pannus in joint spaces with regional inflammation and destruction of articular cartilage and subchondral bone.[4]

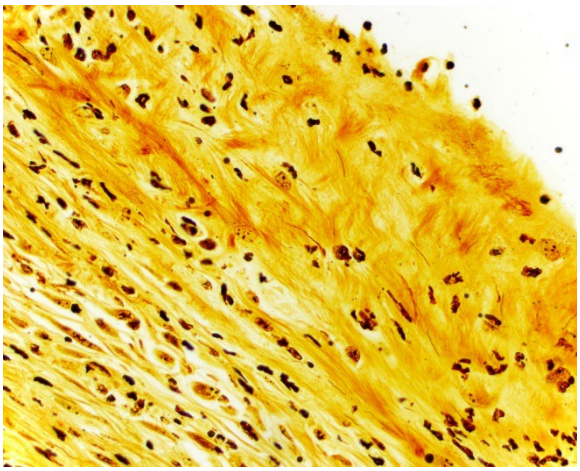

Figure 4-3. Tibiotarsal joint, mouse. Representative high magnification photomicrograph of the tibiotarsal joints from a SCID mouse in which silver impregnated spirochetes are frequently visualized in the inflamed synovium. Warthin-Starry stain. (Warthin Starry 4.0, 400X) (*Photo courtesy of:* Memorial Sloan Kettering Cancer Center, The Rockefeller University, Weill Cornell Medicine. https://www.mskcc.org/research/ski/core-facilities/comparative-medicine-pathology-0)

The use of mouse strains deficient in component of the acquired immune system have been instrumental to understand their role in host defense against *Bb* infection. Several studies have demonstrated the importance of B cell activation and immunoglobulin production in the control of *Bb* infection *in vivo*. (6, 13, 20) Mice deficient antibody production, such as $\mu MT^{-/-}$ mice (lack B cells but bear T cells) and SCID and $rag1^{-/-}$ mice (lack B and T cells) developed persistent tenosynovitis and carditis and exhibited an elevated bacterial burden in tissues. (6, 13, 20) In contrast, studies with mice lacking all T cells (TCR $\beta/\delta^{-/-}$) or only αβ TCR-expressing cells, or with mice depleted of CD4 or CD8 T

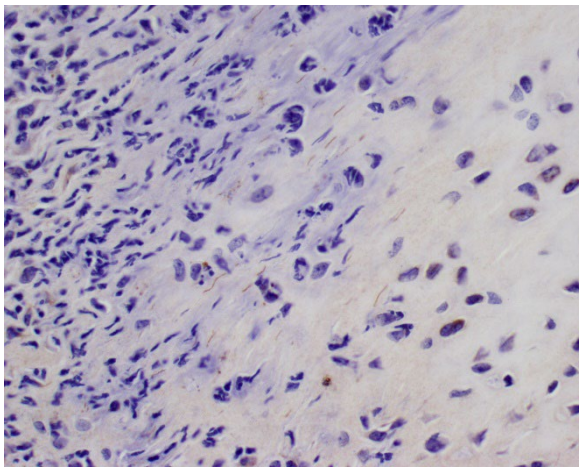

Figure 4-4. Tibiotarsal joint, mouse. Representative high magnification photomicrograph of the tibiotarsal joints from a SCID mouse in which spirochetes are detected in the inflamed synovium and periosteum. (anti-*B. burgdorferi*, 400X) (*Photo courtesy of:* Memorial Sloan Kettering Cancer Center, The Rockefeller University, Weill Cornell Medicine. https://www.mskcc.org/research/ski/core-facilities/comparative-medicine-pathology-0)

cells, have shown a minor role for T cell-deficiency during course of *Bb* infection. (20)

The signaling pathway involved for the enhanced severity of tenosynovitis in C3H mice was identified by global gene expression analysis in *Bb*-infected tibiotarsal joints. Miller et al., demonstrated that type I interferons were upregulated in the tibiotarsal joints of C3H mice at 1 week of *Bb* infection, 2-3 weeks prior the development of subacute tenosynovitis in this mouse.[14,15] The peak of type I interferons (IFN-α/β) likely occurred prior to infiltration of lymphocytes into the joints lesions of C3H mice.[14,20] The involvement of type I interferons in tenosynovitis was subsequently confirmed by either the systemic administration of a type I interferon receptor (IFNAR-1) blocking antibody or the ablation of the IFNAR1 in mice, which resulted in suppression of type 1 interferons and tenosynovitis in tibiotarsal joints of mice.[14,20] The early upregulation of IFN-responsive transcripts was absent in the joints from tenosynovitis resistant C57BL/6 mouse.[14] Instead, *Bb* infected C57BL/6 mice displayed an increased expression in genes involved in epidermal differentiation, cell adhesion, cell-cell interaction, and wound repair.[14,15] Additionally, IL10$^{-/-}$ mice on the C57BL/6 background showed several IFN-inducible transcripts were markedly upregulated in the joints at 2 weeks of infection and exhibited increased tenosynovitis severity.[18] Infected IL-10$^{-/-}$ mice also exhibited upregulation of inflammatory mediators, such as IFN-γ, CXCL9, and CXCL10 and tibiotarsal joints were infiltrated with NK cells, NKT cells, CD4^{+} T cells, and macrophages.[18]

Unlike most classical gram-negative bacterial pathogens, *Bb* does not produce LPS or toxins and lacks a specialized secretory system. Instead, the *Bb* genome encodes numerous surface lipoproteins that allow spirochetes to adapt, adhere, invade, and/or persist in tis sues.[17] These surface proteins are recognized by TLR2 receptor and induce a proinflammatory response via MyD88 signaling pathway.[8,17] In addition, CD14 is a glycosylphosphatidylinositol (GPI)-anchored membrane protein expressed on macrophages/monocytes that serves as a co-receptor for TLR2 to facilitate the activation of the innate immune response against *Bb*.[8] Previous studies have shown that the loss of either TLR2 or CD14 in mice leads to a defective innate immune response against *Bb,* and both TLR2$^{-/-}$ and CD14$^{-/-}$ mice showed an increased severity of tenosynovitis.[5,21] There are several inflammatory mediators, such as prostaglandins, leukotrienes, neutrophil recruiting chemokine (KC) among others, in which the use of targeted gene-knockout mouse strains have demonstrated their role in modulating tenosynovitis in Bb-infected mice.[6,16] In addition, classical forward ge-

netic experiments using intercross populations between C3H and B6 mice led to the identification of multiple *Bb* arthritis–associated (*Bbaa*) quantitative trait loci (QTL) on five different chromosomes of the mouse (chromosome 1, 4, 5, 11 and 12).[19]

Natural bacterial infections resulting in primary arthritis in laboratory mice are rare, but arthritis can occur as result of septicemia and/or local opportunistic bacterial infections in the joints. Septic arthritis has been described in laboratory mice infected with *Streptobacillus moniliformis* and *Corynebacterium kutscheri*.[10] Monoarticular pyogenic arthritis may occur as result of opportunistic bacterial infections due to cutaneous abrasions and lacerations infected with opportunistic bacteria.[10] Bacterial agents that can cause suppurative arthritis in laboratory mice include *Staphylococcus aureus*, Group B *Streptococcus* spp. *Rodentibacter pneumotropica*, *E. coli*, and *Klebsiella pneumoniae* spp. Experimental infections with *Mycoplasma pulmonis* can cause polyarthritis in experimentally inoculated B cell-deficient mice and SCID mice, and immunocompetent C3H/HeN mice.[10] However, arthritis is not a significant feature in natural *M. pulmonis* infections in mice.[10] *M. pulmonis* induced arthritis is characterized initially by suppurative inflammation affecting primarily the carpal and tarsal joints and associated tendon sheaths. As the process becomes chronic, lymphocytic cell infiltration and synovial hyperplasia are common histological features in the affected joints.[10]

Contributing Institution:
Laboratory of Comparative Pathology, Memorial Sloan Kettering Cancer Center, The Rockefeller University, Weill Cornell Medicine.

https://www.mskcc.org/research/ski/core-facilities/comparative-medicine-pathology-0

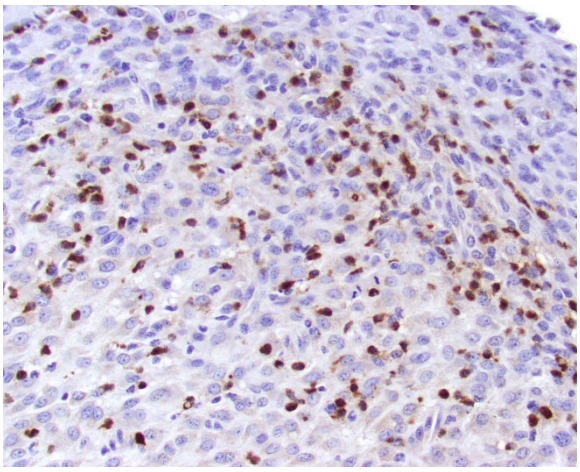

Figure 4-5. Tibiotarsal joint, mouse. Representative immunohistochemistry of the tibiotarsal joint in which moderate to large numbers of Ly6G+ neutrophils are detected in areas of synovial hyperplasia and hypertrophy. (anti-Ly6+, 400X) (*Photo courtesy of:* Memorial Sloan Kettering Cancer Center, The Rockefeller University, Weill Cornell Medicine. https://www.mskcc.org/research/ski/core-facilities/comparative-medicine-pathology-0)

JPC Diagnosis:

Tarsal joint: Tenosynovitis, proliferative and neutrophilic, chronic, diffuse, severe with focal bony lysis and periosteal new bone growth

JPC Comment:
We were excited to finally utilize this case as it has been waiting on our shelf for several years for a moderator willing to jump into the details that are so painstakingly crafted. Experimental disease cases can be difficult to read cold as JPC conference participants only get the tissue and species in advance of the conference date, and a single HE section without access to the special stains that demonstrate the presence and morphology of an infectious agent.

Many conference participants considered neoplasms such as histiocytic sarcoma and osteosarcoma as primary differentials in this case given the involvement of the cortical bone

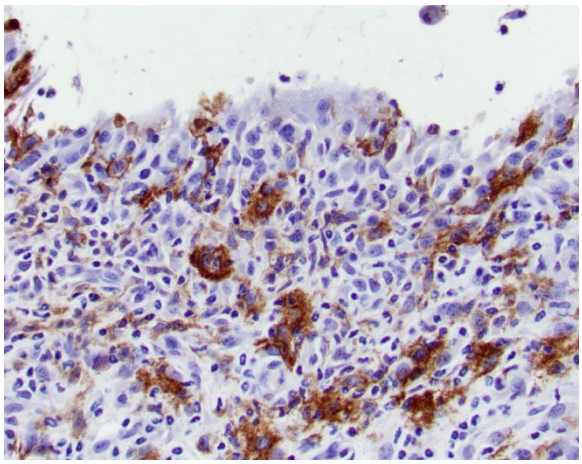

Figure 4-6. Tibiotarsal joint, mouse. Representative immunohistochemistry of the tibiotarsal joint in which moderate to large numbers of Ly6G+ neutrophils are detected in areas of synovial hyperplasia and hypertrophy. (anti-Ly6+, 400X) (*Photo courtesy of:* Memorial Sloan Kettering Cancer Center, The Rockefeller University, Weill Cornell Medicine. https://www.mskcc.org/research/ski/core-facilities/comparative-medicine-pathology-0)

and the extensor tendon. That said, the absence of mitotic figures and matrix and the presence of many neutrophils are more suggestive of granulation tissue than neoplasia. Periosteal new bone formation reflects periosteal irritation and could support either bony infection or neoplasia. Some participants considered the potential for an induced neoplasm (i.e. osteosarcoma) secondary to inflammation, though the role of *Bb* in neoplasia appears to be limited to a short description in certain human breast cancers.[22]

Conference participants also discussed "pannus" in the context of this lesion. "Pannus" describes the spread of fibrovascular or granulation tissue across multiple organs including the cornea, joint surfaces, and the endothelium. In a veterinary context, this can be confusing as chronic superficial keratitis (also referred to as "pannus") is more commonly seen in primary practice than erosive polyarthritis. Additionally, veterinary literature seldom uses the term pannus to describe thickening of the joint and/or bony/cartilaginous involvement in osteoarthritis cases. Murine tissue transplantation, particularly with SCID mice, may be one exception to this observation.[23]

References:

1. Barthold SW, Beck DS, Hansen GM, Terwilliger GA, Moody KD. Lyme borreliosis in selected strains and ages of laboratory mice. *J Infect Dis*. 1990;162: 133-138.
2. Barthold SW. Infectivity of Borrelia burgdorferi relative to route of inoculation and genotype in laboratory mice. *J Infect Dis*. 1991;163: 419-20.
3. Barthold SW, Sidman CL, Smith AL. Lyme borreliosis in genetically resistant and susceptible mice with severe combined immunodeficiency. *Am J Trop Med Hyg*. 1992;47: 605-613.
4. Barthold SW, Cadavid, D., Philipp, M. Animal Models of Borreliosis. S Samuels and J Radolph, In: *Borrelia: Molecular Biology, Host Interaction and Pathogenesis*, 1st edition, Norfolk, UK: Caister Academic Press; 2010:359-411.
5. Benhnia MR, Wroblewski D, Akhtar MN, Patel RA, Lavezzi W, Gangloff SC, Goyert SM, Caimano MJ, Radolf JD, Sellati TJ. Signaling through CD14 attenuates the inflammatory response to Borrelia burgdorferi, the agent of Lyme disease. *J Immunol*. 2005;174:1539-48.
6. Bockenstedt LK, Wooten RM, Baumgarth N. Immune Response to Borrelia: Lessons from Lyme Disease Spirochetes. *Curr Issues Mol Biol*. 2021;42: 145-190.
7. Bosma MJ, Carroll AM. The SCID mouse mutant: definition, characterization, and potential uses. *Annu Rev Immunol*. 1991; 9:323-50.
8. Cervantes JL, Hawley KL, Benjamin SJ,

Weinerman B, Luu SM, Salazar JC. Phagosomal TLR signaling upon Borrelia burgdorferi infection. *Front Cell Infect Microbiol*. 2014; 20; 4:55.
9. de Souza MS, Smith AL, Beck DS, Kim LJ, Hansen GM Jr, Barthold SW. Variant responses of mice to Borrelia burgdorferi depending on the site of intradermal inoculation. *Infect Immun*. 1993;61: 4493-7.
10. Fox J, Barthold S, Davisson M, Newcomer C, Quimby F, Smith A. Bacterial diseases. In: *The Mouse In Biomedical* Research. Vol 2, 2nd edition, San Diego, CA USA: El Sevier Inc; 2006: 325-469.
11. Franklin CL. Microbial considerations in genetically engineered mouse research. *ILAR J*. 2006; 47 :141-55.
12. Ma Y, Seiler KP, Eichwald EJ, Weis JH, Teuscher C, Weis JJ. Distinct characteristics of resistance to Borrelia burgdorferi-induced arthritis in C57BL/6N mice. *Infect Immun*. 1998;66: 161-168.
13. McKisic MD, Redmond WL, Barthold SW. Cutting edge: T cell-mediated pathology in murine Lyme borreliosis. *J Immunol*. 2000;164: 6096-6099.
14. Miller JC, Ma Y, Bian J, et al. A critical role for type I IFN in arthritis development following Borrelia burgdorferi infection of mice. *J Immunol*. 2008;181: 8492-8503.
15. Miller JC, Ma Y, Crandall H, Wang X, Weis JJ. Gene expression profiling provides insights into the pathways involved in inflammatory arthritis development: murine model of Lyme disease. *Experimental and Molecular Pathology*. 2008;85: 20-27
16. Pratt CL, Brown CR. The role of eicosanoids in experimental Lyme arthritis. *Front Cell Infect Microbiol*. 2014; 28:4:69.
17. Radolf JD, Caimano MJ, Stevenson B, Hu LT. Of ticks, mice and men: understanding the dual-host lifestyle of Lyme disease spirochaetes. *Nat Rev Micro*. 2012;10: 87-99.
18. Sonderegger FL, Ma Y, Maylor-Hagan H, et al. Localized production of IL-10 suppresses early inflammatory cell infiltration and subsequent development of IFN-gamma-mediated Lyme arthritis. *J Immunol*. 2012;188: 1381-1393.
19. Weis JJ, McCracken BA, Ma Y, et al. Identification of quantitative trait loci governing arthritis severity and humoral responses in the murine model of Lyme disease. *J Immunol*. 1999;162: 948-956
20. Weis JJ, Bockenstedt, L.K. Host Response. In: *Borrelia: Molecular Biology, Host Interaction and Pathogenesis*. 1st edition. Norfolk, UK: Caister Academic Press; 2010:413-441.
21. Wooten RM, Ma Y, Yoder RA, Brown JP, Weis JH, Zachary JF, Kirschning CJ, Weis JJ. Toll-like receptor 2 is required for innate, but not acquired, host defense to Borrelia burgdorferi. *J Immunol*. 2002; 168:348-55.
22. Gaur G, Sawant JY, Chavan AS, et al. Effect of Invasion of Borrelia burgdorferi in Normal and Neoplastic Mammary Epithelial Cells. *Antibiotics (Basel)*. 2021 Oct 24;10(11):1295.
23. Liu S. Human Xenograft Model. *Methods Mol Biol*. 2024;2766:9-15.